A connection of winter Eurasian cold anomaly to the modulation of Ural blocking by ENSO

Binhe Luo[a,b], Dehai Luo[b], Aiguo Dai[c], Ian Simmonds[d], and Lixin Wu[a]

(a) Key Laboratory of Physical Oceanography/Institute for Advanced Ocean Studies, Ocean University of China and Qingdao National Laboratory for Marine Science and Technology, Qingdao, China

(b) Key Laboratory of Regional Climate-Environment for Temperate East Asia, Institute of Atmospheric Physics，Chinese Academy of Sciences, Beijing, China, 100029 and University of Chinese Academy of Sciences, Beijing, China.

(c) Department of Atmospheric and Environmental Sciences, University at Albany, SUNY, Albany, NY 12222, USA

(d) School of Geography Earth and Atmospheric Sciences, University of Melbourne, Melbourne, Victoria, Australia

This is the author manuscript accepted for publication and has undergone full peer review but has not been through the copyediting, typesetting, pagination and proofreading process, which may lead to differences between this version and the Version of Record. Please cite this article as doi: 10.1029/2021GL094304.

Abstract

This study investigates how El Niño-Southern Oscillation (ENSO) modulates winter cold anomalies over central Eurasia using reanalysis data during 1950-2019. It is found that ENSO can significantly influence winter air temperature over central Eurasia mainly through modulating the strength and location of the cyclonic anomaly of Ural blocking (UB) or long-lived UB events. A strong (weak) cyclonic anomaly of UB on the southeastern (eastern) side of the Ural Mountains tends to occur over midlatitude (high-latitude) Eurasia during La Niña (El Niño) winters. Such anomalous circulation leads to a strong (weak) cold anomaly over central Eurasia, especially over East Asia, due to enhanced (weakened) cold air advection toward the central Eurasia during La Niña (El Niño). The UB-related cyclonic anomaly in the midlatitude (high latitude) side of Eurasia is shown to be related to weakened (enhanced) eastward extension of strong westerly winds over midlatitude Eurasia during La Niña (El Niño) winters.

Plain Language Summary

Observations show that in recent decades a strong cold anomaly appears over Eurasia, especially over central Eurasia. This cold anomaly shows notable variations on interannual, decadal and interdecadal timescales. However, what factors lead to its interannual variations is not well understood. Here we show that El Niño-Southern Oscillation (ENSO) events can influence Eurasian winter air temperature by modulating the strength and location of the cyclonic anomaly of Ural blocking or the frequency of long-lived UB events. A La Niña (El Niño) favors a strong (weak) cyclonic anomaly circulation located in the southeastern (eastern) side of the Ural Mountains in the midlatitudes (high latitudes), which leads to a strong (weak) cold anomaly over central Eurasia especially in the low latitude Eurasia (i.e., East Asia) through enhanced (weakened) cold air advection. These new results help us understand the physical cause of the interannual variability of the Eurasian cold anomaly modulated by ENSO.

1. Introduction

Accompanied with the global warming, strong cold events in winter (December-February, DJF) have been observed to occur frequently over central Eurasia (CE) and Siberia in the recent decades (Cohen et al. 2014; Mori et al. 2014, B. Luo et al. 2019). The winter Eurasian cold anomaly (ECA) shows not only clear interdecadal variability, but also notable interannual variations. Although the ECA's interdecadal variations are shown to be related to the Interdecadal Pacific Oscillation (IPO; Dai et al. 2015) and Atlantic Multidecadal Oscillation (AMO; Steinman et al. 2015; Luo et al. 2017; Sung et al. 2018; Jin et al. 2020), less attention has been focused on determining the physical cause of its interannual variations. Given its connection to IPO, which represents the decadal variability in El Niño–Southern Oscillation (ENSO) activity (Dong et al. 2018), it is natural to suspect that ECA's interannual variability may be linked to ENSO. However, whether such a link actually exists and how it is formed are unknown.

Many previous studies using atmospheric reanalysis and model data have revealed that atmospheric internal modes, such as atmospheric blocking, the Pacific-North American (PNA) pattern and the North Atlantic Oscillation (NAO), are modulated by ENSO (Wiedenmann et al. 2002; Müller and Roeckner 2006; Li and Lau 2012). For example, blocking events in the Northern Hemisphere are more frequent during La Niña winters than during El Niño winters (Wiedenmann et al. 2002). Some studies also found that the positive (negative)-phase NAO [NAO^+ (NAO^-)] events or the negative (positive) PNA events are associated with the negative (positive) phase of ENSO (Lin et al. 2005; Müller and Roeckner 2006; Li and Lau 2012). While the ENSO modulates the North American weather and climate via the changes in the PNA

(Straus and Shukla 2002; Li et al. 2019) and North Pacific Oscillation (Guan et al. 2020), it can also influence the winter Eurasian climate and weather through stratospheric processes (Butler et al. 2014).

Because Ural blocking (UB) plays a key role in the formation of winter ECA (Luo et al. 2016a-b, Yao et al. 2017, B. Luo et al. 2019, Li et al. 2021), it is speculated that ENSO influences winter ECA probably through its modulation of UB due to the change of winter Eurasian midlatitude zonal winds (Luo et al. 2019), even though the ENSO's negative phase favors Ural-Siberian blocking (Cheung et al., 2012). This would be in addition to the Arctic influence on winter Eurasian temperature variability through the Arctic Amplification (AA) and Arctic Oscillation (AO) (Kim and Son 2016, Screen et al. 2018), although European temperature variability has already been linked to El Niño (Ineson and Scaife, 2009; López-Parages et al. 2015). In this study, we analyze atmospheric reanalysis data to show that the ENSO can significantly influence winter ECA through its modulation of the strength and location of the cyclonic anomaly of UB or the frequency of long-lived UB events. These results can improve our understanding of the cause of winter cold anomalies over central Eurasia on interannual timescales.

2. Data and Method

We used the daily data on a 2.5^{o} grid taken from the National Centers for Environmental Prediction/National Center for Atmospheric Research (NCEP/NCAR) reanalysis for winter (December and February, DJF) during the period from December /1950/February 1951 to December 2019/February 2020 (1950-2019 winter hereafter) (Kalnay et al. 1996; https://psl.noaa.gov/data/gridded/data.ncep.reanalysis.html). The data include surface air temperature (SAT), 500-hPa geopotential height (Z500) and zonal wind (U500), 850-hPa horizontal wind (U850, V850). We used DJF-mean Niño3.4 index − the SST anomaly averaged over 170°-120°W, 5°S-5°N − as the ENSO index, which was taken from the Koninklijk Nederlands Meteorologisch Instituut (KNMI) Climate Explorer (http://climexp.knmi.nl/selectindex.cgi?id=someone@somewhere). All data were converted into anomalies by removing the 1950-2019 mean, and the decadal variations of 9 years or greater were removed from the ENSO index and winter SAT anomalies by removing the 9-year moving average to focus on the interannual-to-multiyear variations. Winters with the 9-year (or 9-yr) high pass Niño 3.4 index above 0.5 (below -0.5) standard deviations (STDs) are defined as the El Niño (La Niña) winters. Other values are defined as the ENSO neutral winters.

To identify Ural blocking in the region from 40°-80°E, we used the one-dimensional blocking index of Tibaldi and Molteni (1990, TM hereafter) based on the reversal of the meridional Z500 gradient: GHGN=$\frac{Z500(\phi_N)-Z500(\phi_o)}{\phi_N-\phi_o}$ and GHGS=$\frac{Z500(\phi_o)-Z500(\phi_s)}{\phi_o-\phi_s}$ at three given latitudes $\phi_N = 80^oN + \Delta$, $\phi_o = 60^oN + \Delta$, $\phi_s = 40^oN + \Delta$ and $\Delta = -5^o, 0^o, 5^o$. A large-scale blocking event is detected if the GHGS > 0 and GHGN < -10 gpm (deg lat)$^{-1}$ conditions are satisfied in a longitudinal domain at least of 15° longitudes for a given minimum duration threshold (the number of consecutive days) of blocking and for at least one choice of the Δ values. Although the TM index is different from that of Pelly and Hoskins (2003, PH), in our calculation we added the same large-scale blocking condition as used in PH. Diao et al. (2006) have evaluated the difference of the identified blocking between the TM and PH indices and found that their results are similar. When the used TM index is confined in the domain 40°-80°E, the identified blocking event is the Ural blocking (UB) as in Luo et al (2016a) and Yao et al. (2017). Here, to ensure that there are enough UB events in our calculation, we use 3 days as a minimum duration threshold of blocking. We also examine the sensitivity of our result to the choice of the duration threshold. It is found that our result does not strongly depend on the minimum duration threshold of blocking. For example, for a minimum blocking duration threshold of 4 days the obtained result is similar and shown in the Supporting Information file.

We used a two-sided Student t-test to determine the statistical significance of the anomaly or the difference between two fields at each grid point. This statistical method is described in Wilks (2011).

3. Results

3.1 Winter Eurasian cold anomaly and its linkage to the phase of ENSO

Calculation indicates that the DJF-mean SAT anomaly averaged over central Eurasia (60°-120°E, 40°-60°N; CE), as denoted by T_{CE}, shows a considerable interannual variability (Fig.S1a in the Supporting Information file). Regressed DJF-mean SST anomaly against the 9-yr high pass DJF-mean T_{CE} time series $\times(-1.0)$ shows that the winter cold anomaly over CE corresponds to a La Nina-like SST anomaly pattern in the equatorial Pacific (Fig. S1b), thus indicating that the interannual variability of the Eurasian cold anomaly (ECA) is linked to ENSO, even though it is modulated by the North Atlantic SST anomaly. We also see that the strong winter ECA corresponds to a negative Arctic Oscillation (AO^-) (Cheung et al. 2012) that resembles a combination of both UB and the negative phase (NAO^-) of the North Atlantic Oscillation (NAO) (Fig. S1c). In the AO^- pattern, its Atlantic component like an NAO^- is related to the warm-cold-warm tripole SST anomaly over North Atlantic (Czaja and Frankignoul, 2002). Thus, the strong Eurasian cold anomaly is not only related to Ural blocking, but also related to the La Niña-like SST anomaly and the North Atlantic warm-cold-warm tripole SST pattern. However, it does not imply that a La Nina-like SST anomaly can produce a combined pattern of NAO^- and UB.

In fact, Müller and Roeckner (2006) revealed a negative correlation between the ENSO and NAO. As a consequence, the La Nina favors a positive NAO (NAO^+) pattern (Fig. S2), consistent with the result of Li and Lau (2012). For this case, La Nina also corresponds to a positive Z500 anomaly near Ural Mountains and a cold anomaly in the middle to low latitudes of Eurasia. But a strong cold anomaly is seen in the high latitude Eurasia for the NAO^- (Fig. S1c), even when UB is present. Thus, the ENSO may be one of factors influencing the winter Eurasian cold anomaly. Because the ENSO influences the winter air temperature and wind field over Eurasia via stratospheric processes (Butler et al. 2014), it is speculated that it can influence the ECA probably through change of UB due to the change in the winter zonal winds. In this paper, we do not consider the roles of the North Atlantic SST anomalies (or the phase of NAO) and stratospheric processes in modulating the ECA. Instead, we focus on different impacts of El Nino and La Nina on the interannual variability of ECA via the UB change. As we will see later, a strong cold anomaly associated with La Niña mainly occurs in the southern part of CE.

It is useful to show the time series of the 9-yr high pass filtered DJF-mean Niño 3.4 index during 1950-2019 in Fig. 1a. Using the 0.5 STD threshold, it is found that there are 23 La Niña, 27 neutral and 20 El Niño winters during 1950-2019. The composite DJF-mean Z500 and SAT anomalies for the La Niña and El Niño winters are shown in Figs. 1b-c. We note that during the La Niña winters there is a strong cold anomaly of 0.5-1.5K mainly in the southern part of

CE and a strong warm anomaly of 1.0-2.0K over the BKS, and the SAT anomaly pattern concurs with a large-scale high (low) pressure anomaly in the north (south) of 50°N (Fig. 1b). A strong cold anomaly can even appear in the low latitude Eurasia especially over East Asia including China, Korea and Japan in this case. In contrast, the cold anomaly disappears over CE during the El Niño winters, replaced by a reversed, southward-shifted meridional dipole pattern with weak SAT and Z500 anomalies within 60°-90°E (Fig. 1c). As seen from Fig. 1d, a strong cold anomaly is more prevalent in the south of 50°N during La Niña than during El Niño. A similar result is found for a strong ENSO phase with 1.0 STDs (not shown). While an intense warm anomaly could occur over CE for a strong El Niño, a strong cold anomaly mainly appears in the southern CE for a strong La Niña.

Moreover, we see that the DJF-mean Z500 anomaly during the La Niña winters shows an anticyclonic anomaly located in the Ural Mountains and in the east of 60°E (Fig. 1b), which resembles a winter high-latitude blocking pattern over the Ural-Siberia region, whose anticyclonic center is a little in the higher latitudes than that of the climatological mean UB (Luo et al. 2016a). Thus, it is of significance to examine the contribution of UB events to the cold anomaly over CE during the La Niña and El Niño winters. When the daily Z500 and SAT anomalies associated with UB events (the days from lag -10 to 10 days) are removed, the composite DJF-mean SAT anomaly shows a warm anomaly over CE during both La Niña winters and El Niño winters (Fig. S3). This suggests that UB plays a crucial role for producing the winter cold anomaly over CE during the La Niña winters. Below, we further examine how the ENSO influences the sub-seasonal cold anomaly over CE through changing UB.

3.2 Characteristics of the UB and sub-seasonal ECA during different ENSO phases

Our analysis shows that there are 46, 42 and 39 UB events for a minimum blocking duration threshold of 3 days during La Niña, neutral and El Niño winters during 1950-2019, which correspond to 2.0, 1.56 and 1.95 UB events per winter, respectively. For a minimum blocking duration threshold of 4 days, there are 38, 34 and 33 UB events during La Niña, neutral and El Niño winters, which correspond to 1.65, 1.26 and 1.65 UB events per winter, respectively. Clearly, the ENSO does not significantly modulate the frequency of UB events, while it can modulate the frequency of long-lived UB events as noted below. We show the time-mean fields of the composite daily Z500 and SAT anomalies and 850-hPa wind vectors averaged from lag -10 to +10 days (lag 0 denotes the peak day of blocking) of the UB events in Figs. 2a-c for the La Niña, neutral and El Niño winters, and the time-longitude evolutions of their composite daily Z500 anomalies averaged over 50^o-70^oN in Figs. 2d-f. It is found that La Niña and El Niño correspond to high-latitude UBs, even though the anticyclonic center of UB is slightly stronger (located slightly more north) during La Niña (Fig. 2a) than during El Niño (Fig.2b). Figure 2a also shows a strong sub-seasonal cold anomaly over CE and East Asia during the UB events accompanied by a strong positive Z500 anomaly to the north and a strong negative Z500 anomaly to the south in the La Niña phase. The negative Z500 anomaly is relatively strong and its cyclonic center is located near 47^oN and 90^oE in the southeast of Ural Mountains. The presence of the anti-cyclonic anomaly circulation would enhance cold advection (green vector in Fig. 2a) from the Arctic to CE and East Asia through combining the strong cyclonic circulation anomaly in the southeast of the Ural Mountains over the midlatitudes. Compared to the role of AO^- or NAO^- (Cheung et al. 2012), the UB-related sub-seasonal Eurasian cold anomaly during La Niña is mainly located in a relatively low latitude region of Eurasia including East Asia (China, Korea and Japan).

In contrast, a weak cold anomaly is seen over CE together with a weakened negative height anomaly to the south for the neutral and El Niño phases (Fig.2b-c). During the El Niño phase, the cyclonic anomaly of the UB is relatively weak and its cyclonic center is located at 52°N and 120°E mainly in the eastern side of the Ural Mountains over the high latitudes (Fig. 2c). This orientation is not conducive for a strong cold anomaly to form over CE owing to the absence of strong cold advection from Arctic to CE. It is noted that the differences of the strength and location of the anticyclonic anomaly of UB between El Niño and La Niña phases are smaller than those of the UB cyclonic anomaly. However, the strength and location of the large-scale cyclonic anomaly of UB are important for whether a strong sub-seasonal cold anomaly occurs over CE, which are significantly modulated by La Niña and El Niño. A strong (weak) sub-seasonal cold anomaly over CE is associated with the strong (weak) cold air advection toward central Eurasia due to the presence of a large-scale midlatitude (high latitude) cyclonic anomaly of the UB in the southeast (east) of the Ural Mountains during the La Niña (El Niño) phase (Figs.2a, c). A similar result is found for a minimum blocking duration threshold of 4 days (Fig. S4).

It is also seen from Figs. 2d-f that the UB shows slow westward movement (less movement) during the La Niña (El Niño) phase. In the time-mean field of composite daily Z500 anomaly, the anticyclonic center of UB is located more east during the La Niña winter (Fig.2a) than during the El Niño winter (Fig. 2c) possibly because the initial UBs mostly originate from the east of 60°E for the La Niña (Fig. 2d) and the winter zonal wind near 60°N and 60°E is slightly stronger during La Niña than during El Niño (Fig. 3f, below). The duration of blocking (persistence days with at least 80 gpm height anomaly) during the La Niña phase is about 9 days and a little longer than the duration (~8 days) of UB during the El Niño phase (Figs. 2d, f), although their blocking duration difference is not statistically significant at $p<0.1$. Thus, the ENSO mainly modulate the strength and location of the cyclonic anomaly of UB, even though the duration of UB and its anticyclonic anomaly are slightly influenced by ENSO. Our investigation shows that there are 15, 8 and 9 long-lived (⩾9 days) UB events during La Niña, Neutral and El Niño winters, which correspond to 33% (15/46), 19% (8/42) and 23% (9/39) of the total UB events. Thus, La Niña more favors long-lived UB events than does El Niño. A daily composite of UB events based on the peak day (lag 0) of UB also reveals that during the La Niña winter the UB often occurs together with a positive NAO (NAO^+) (Fig. S5) and the NAO^+ is relatively strong compared to other cases before the UB matures. This is because the La Niña favors NAO^+ (Li and Lau, 2012). Thus, the NAO^+ is a precursor of the UB formation (Luo et al. 2016b). To some extent, the ENSO modulates the winter cold anomaly over CE mainly through changing the strength and location of the large-scale cyclonic anomaly of UB and the frequency of long-lived UB events.

3.3 Physical cause of ENSO's Impact on UB and associated sub-seasonal cold anomaly

Previous studies have revealed that the ENSO can force the PNA pattern to influence the North American weather and climate (Straus and Shukla 2002; Li et al 2019), and it can also change northern midlatitude winter background state through a stratospheric pathway (Butler et al. 2014). Butler et al. (2014) noted that the difference of the winter temperature anomaly between El Niño and La Niña corresponds to a negative (positive) anomaly to the north (south) of 50^{o}N over Eurasia, thus implying that El Nino corresponds to stronger midlatitude zonal winds over Eurasia than La Nina. However, they did not present the distribution of winter zonal winds. Here, we explore the difference of the winter background zonal wind over Eurasia between El Niño and La Niña phases to further examine the mechanism of the influence of the ENSO on the UB.

We show the DJF-mean SAT, Z500 and U500 anomalies excluding the days with UB events for the La Niña and El Niño phases and their differences in Fig.3. It is found that in the absence of UB events a winter cyclonic anomaly exists over the Ural Mountains north of 50^{o}N, which is stronger during the El Niño phase than during the La Niña phase (Figs. 3a-b), even though there is a strong cyclonic-over-anticyclonic dipole anomaly centered around 50^{o}N along the Ural Mountains and its downstream side during the El Niño and La Niña phases. Figure 3d-f show that winter U500 over midlatitude central-East Asia is stronger during the El Niño than La Niña phase (Fig. 3d-e), as also seen from their difference (Fig. 3f). In other words, strong winter westerly winds show a small (large) eastward extension in the Eurasian midlatitudes during the La Niña (El Niño) phase. Such winter midlatitude U500 difference change between El Niño and La Niña phases are related to the stratospheric influence, as noted by Butler et al. (2014). Thus, a strengthened midlatitude zonal wind during the El Niño phase favors the eastward migration of the cyclonic anomaly of UB, which can lead to the cyclonic anomaly of UB being weaker and located in the higher latitude region to the east of Ural Mountains than during the La Niña phase. Such a UB structure offsets some of the northeasterly winds caused by the UB anticyclonic anomaly (Fig. 2c), resulting in weaker cold advection from the northeast, opposite to that during the La Niña phase. This explains why the El Niño phase is not favorable for the generation of strong winter cold anomaly over CE during the UB episode.

4. Summary and discussion

In this paper, we have investigated the impact of the ENSO on the winter cold anomaly over central Eurasia (40º-60ºN, 60º-120ºE; CE) through modulating Ural blocking (UB). It is found that the ENSO influences the sub-seasonal cold anomaly over CE mainly through changing the strength and location of the cyclonic anomaly of UB and the frequency of long-lived UB events. During the La Niña phase, a strong large-scale cyclonic anomaly of UB occurs in the Eurasian midlatitudes and is located in the southeast of the Ural Mountains, thus leading to a strong sub-seasonal cold anomaly over the south of CE that influences low latitude Eurasia and East Asia (i.e., China, Korea and Japan) through intensified southward cold air advection. In this case, the Eurasian cold anomaly during the UB episode is usually located in lower latitudes than the combined NAO^- and UB pattern or AO^-. In contrast, during the El Niño phase the cyclonic anomaly of UB is weak and located in the high latitudes to the farther east of Ural Mountains, thus leading to the weak cold anomaly over CE due to weakened southward cold air advection from Arctic. The physical mechanism of the ENSO affecting the strength and location of the large-scale cyclonic anomaly of UB is further explored. It is revealed that the presence of a strong (weak) large-scale cyclonic anomaly of UB in the southeast (east) of Ural Mountains in the midlatitudes (high latitudes) is likely related to reduced (intensified) eastward extension of relatively strong mid-latitude winter westerly winds over Eurasia during the La Niña (El Niño) phase. The change of the winter Eurasian midlatitude zonal winds between La Niña and El Niño is associated with the different stratospheric influence (Butler et al. 2014), which leads to intensified (weakened) eastward mid-latitude winter westerly winds over

Eurasia during El Niño (La Niña) as shown in Fig.3d-f. As a result, intensified midlatitude winter westerly winds during El Niño promote the eastward shift of the cyclonic anomaly of UB and inhibit its strength so that the cyclonic anomaly of UB is weaker and located more east in the high latitude Eurasia than during La Niña. Thus, the winter zonal wind difference leads to the difference of the cyclonic anomaly of UB in its strength and location between El Niño and La Niña.

It should be pointed out that in this paper we only consider the impact of the ENSO on the Eurasian cold anomaly on interannual timescales. Because the Pacific Decadal Oscillation (PDO) or the Interdecadal Pacific Oscillation (IPO)-induced SST anomaly patterns are comparable to those of ENSO (Dong et al. 2018), it is possible that the POD/IPO may influence the Eurasian winter temperatures on decadal time scales through similar processes as discussed here. This requires further investigation.

Acknowledgements

This research was supported by the National Natural Science Foundation of China (Grant numbers: 41790473), the Chinese Academy of Sciences Strategic Priority Research Program (Grant XDA19070403) and National Key research and Development Program of China (2016YFA0601802). The NCEP-NCAR reanalysis data is available from https://psl.noaa.gov/data/gridded/data.ncep.reanalysis.html, the Niño3.4 indices are available from http://climexp.knmi.nl/selectindex.cgi?id=someone@somewhere.

References:

Butler, A., Polvani, L. and C. Deser, 2014: Separating the stratospheric and tropospheric pathways of El Niño–Southern Oscillation teleconnections. *Environ. Res. Lett.,* 9, 024014 (9pp).

Cheung, H. N., W. Zhou, H. Y. Mok, and M. Wu, 2012: Relationship between Ural-Siberian blocking and the East Asian winter monsoon in relation to the Arctic Oscillation and the El Niño–Southern Oscillation. *J. Climate,* 25, 4242–4257, https://doi.org/10.1175/JCLI-D-11-00225.1.

Cohen, J., and Coauthors, 2014: Recent Arctic amplification and extreme mid-latitude weather. *Nat. Geosci.,* **7,** 627–637, https://doi.org/10.1038/ngeo2234.

Czaja, A. and C. Frankignoul, 2002: Observed impact of Atlantic SST anomalies on the North Atlantic Oscillation, *J. Climate*,**15**, 606–23

Dai, A., J. C. Fyfe, S.-P. Xie, and X. Dai, 2015: Decadal modulation of global surface temperature by internal climate variability. *Nat. Climate Change,* **5**, 555–559, https://doi.org/ 10.1038/nclimate2605.

Dong, B., A. Dai, M. Vuille, and O. Elison Timm, 2018: Asymmetric modulation of ENSO teleconnections by the Interdecadal Pacific Oscillation. *J. Climate*, **31,** 7337-7361. https://doi.org/10.1175/JCLI-D-17-0663.1.

Guan, W. N., X. N. Jiang, X. J. Ren, G. Chen, P. Lin, and H. Lin, 2020: The leading intraseasonal variability mode of wintertime surface air temperature over the North American sector. *J. Climate*, **33,** 9287-9306.

Ineson, S., and A. A. Scaife, 2009: The role of the stratosphere in the European climate response to El Niño. *Nat. Geosci.,* 2, 32–36, doi:10.1038/ngeo381.

Kalnay, E., and Coauthors, 1996: The NCEP/NCAR 40-Year Reanalysis project. *Bull. Amer. Meteor. Soc.,* **77**, 437–471, https://doi.org/10.1175/1520-0477(1996)077,0437: TNYRP. 2.0.CO;2.

Kim K.Y. and S. W. Son, 2016: Physical characteristics of Eurasian winter temperature variability. *Environ. Res. Lett.,* 11, 044009. https://doi.org/10.1088/1748-9326/11/4/044009.

Li, M. et al., 2021: Anchoring of atmospheric teleconnection patterns by Arctic Sea ice loss and its link to winter cold anomalies in East Asia. *Int. J. Climatol.*, **41**, 547–558, doi: 10.1002/joc.6637.

Li, Y. and N. C. Lau, 2012: Impact of ENSO on the atmospheric variability over the North Atlantic in late winter—Role of transient eddies, *J. Climate*, **25**, 320-342.

Li, X., Z. Hu, Liang, P. and J. Zhu, 2019: Contrastive influence of ENSO and PNA on variability and predictability of North American winter precipitation. *J. Climate*, **32**, 6271-6284.

Lin, H., J. Derome, and G. Brunet, 2005: Tropical Pacific link to the two dominant patterns of atmospheric variability, *Geophys. Res. Lett.*, 32, L03801, doi:10.1029/2004GL021495.

López-Parages, J., B. Rodríguez-Fonseca, and L. Terray, 2015: A mechanism for the multidecadal modulation of ENSO teleconnection with Europe. *Climate Dyn.*, 45, 867–880, https:// doi.org/10.1007/s00382-014-2319-x.

Luo, D., Y. Xiao, Y. Yao, A. Dai, I. Simmonds, and C. L. E. Franzke, 2016a: Impact of Ural blocking on winter warm Arctic–cold Eurasian anomalies. Part I: Blocking induced amplification. *J. Climate*, 29, 3925–3947, https://doi.org/10.1175/JCLI-D-15-0611.1.

Luo, D., Y. Xiao, Y. Diao, A. Dai, C. L. E. Franzke and I. Simmonds, 2016b: Impact of Ural Blocking on winter Warm Arctic–Cold Eurasian anomalies. Part II: The link to the North Atlantic Oscillation. *J. Climate*, **29**, 3949-3971, doi: 10.1175/JCLI-D-15-0612.1.

Luo, B., L., Wu, D. Luo, A. Dai and I. Simmonds, 2019: The winter midlatitude-Arctic interaction: effects of North Atlantic SST and high-latitude blocking on Arctic sea ice and Eurasian cooling. *Climate Dynamics* **52**:5-6, 2981-3004.

Luo, D. et al., 2019: Weakened potential vorticity barrier linked to recent winter Arctic sea ice loss and midlatitude cold extremes. *J. Climate*, **32**, 4235-4261, doi: 10.1175/JCLI-D-18-0449.1.

Mori, M., M. Watanabe, H. Shiogama, J. Inoue, and M. Kimoto, 2014: Robust Arctic sea-ice influence on the frequent Eurasian cold winters in past decades. *Nat. Geosci*., 7, 869–873, https://doi.org/10.1038/ngeo2277.

Müller, W. A., and E. Roeckner (2006), ENSO impact on midlatitude circulation patterns in future climate change projections, *Geophys. Res. Lett*., 33, L05711, doi:10.1029/ 2005GL025032.

Screen, J. A. et al., 2018: Polar climate change as manifest in atmospheric circulation. *Current*

Climate Change Reports, **4**, 383-395, doi: 10.1007/s40641-018-0111-4

Steinman, B. A M. E. Mann, and S. K. Miller, 2015: Atlantic and Pacific mul- tidecadal oscillations and Northern Hemisphere temperatures. Science, 347, 988–991, https://doi.org/10.1126/science.1257856.

Straus, D. M. and J. Shukla, 2002: Does ENSO force the PNA? *J. Climate*, 15, 2340-2358.

Sung, M., S. Kim, B. Kim, and Y. Choi, 2018: Interdecadal Variability of the warm Arctic and cold Eurasia pattern and Its North Atlantic origin. *J. Climate*, 31, 5793–5810, https:// doi.org/10.1175/JCLI-D-17-0562.1

Wiedenmann, J. M., A. R. Lupo, I. I. Mokhov, and E. Tikhonova, 2002: The climatology of blocking anticyclones for the Northern and Southern Hemispheres: Block intensity as a diagnostic. *J. Climate*, 15, 3459–3473.

Tibaldi, S., and F. Molteni, 1990: On the operational predictability of blocking. *Tellus*, 42A, 343–365, doi:10.1034/j.1600-0870.1990.t01-2-00003.x.

Yao, Y., D. Luo, A. Dai, and I. Simmonds, 2017: Increased quasi stationarity and persistence of winter Ural blocking and Eurasian extreme cold events in response to Arctic warming. Part I: Insights from observational analyses. *J. Climate*, 30, 3549–3568.

Figure caption:

Figure 1. (a) Time series of the 9-year high pass DJF-mean Niño3.4 index from 1950-2019. The dashed lines represent ±0.5 standard deviations (STDs). (b, c) Composite DJF-mean Z500 (contours, contour interval (CI)=5 gpm) and SAT (color shading, unit in K) anomalies for La Niña (23 cases) and El Niño (20 cases) years. The dots indicate the SAT anomalies are above the 95% confidence level based on a two-sided Student t-test

Figure 2. Time-mean composite daily Z500 (contours, CI=20 gpm) and SAT (color shading, unit in K) anomalies averaged from lag -10 to 10 days (where lag 0 denotes the peak day of blocking) of the 46, 42 and 39 UB events for (a) 23 La Niña, (b) 27 neutral and (c) 20 El Niño winters during 1950-2019, where the green arrow represents the 850-hPa horizontal wind (U850, V850) vector. (d, e, f) Time-longitude evolutions of the composite daily Z500 anomalies (Unit: gpm) averaged over 50^{o}-70^{o}N for the (d) La Niña, (e) neutral and (f) El Niño winters during 1950-2019. The color shading anomalies in panels a-c are above the 95% confidence level based on a two-sided Student *t*-test.

Figure 3. Composite DJF-mean (a, b) Z500 (contours, CI=5 gpm) and SAT (color shading, unit in K), and (d, e) U500 anomalies (m/s) for days without UB events (i.e., blocking days from lag -10 to 10 days being removed) for (a, d) La Niña and (b, e) El Niño winters during

1950-2019, and (c, f) the El Niño minus La Niña difference. Dots indicate the colored anomalies being above the 95% confidence level based on a two-sided Student t-test.

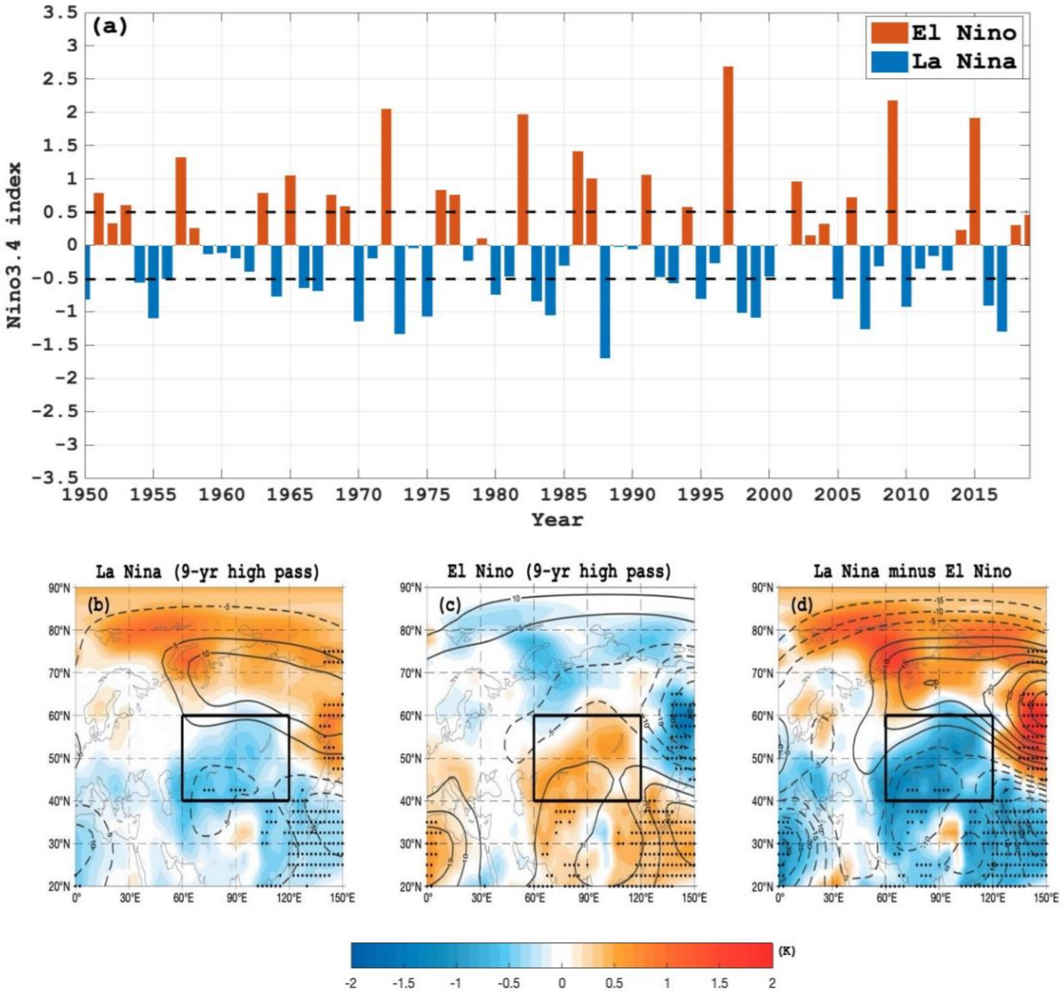
(a)
El Nino
La Nina
Nino3.4 index
Year
La Nina (9-yr high pass)
(b)
El Nino (9-yr high pass)
(c)
La Nina minus El Nino
(d)
(K)

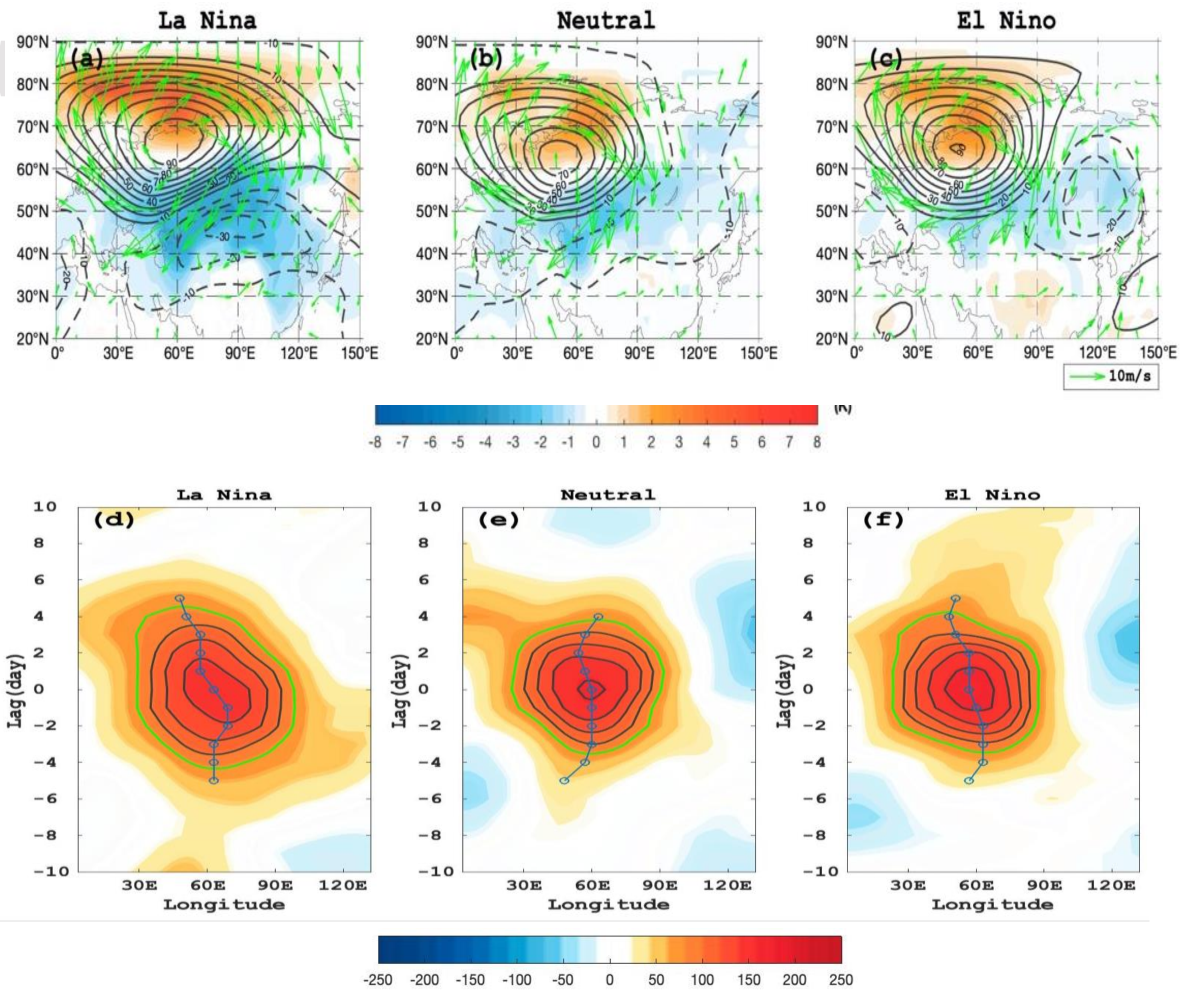
La Nina
Neutral
El Nino
(a)
(b)
(c)
90°N
80°N
70°N
60°N
50°N
40°N
30°N
20°N
0°
30°E
60°E
90°E
120°E
150°E
10m/s
-8 -7 -6 -5 -4 -3 -2 -1 0 1 2 3 4 5 6 7 8
(d)
(e)
(f)
Lag(day)
Longitude
30E
60E
90E
120E
-250 -200 -150 -100 -50 0 50 100 150 200 250

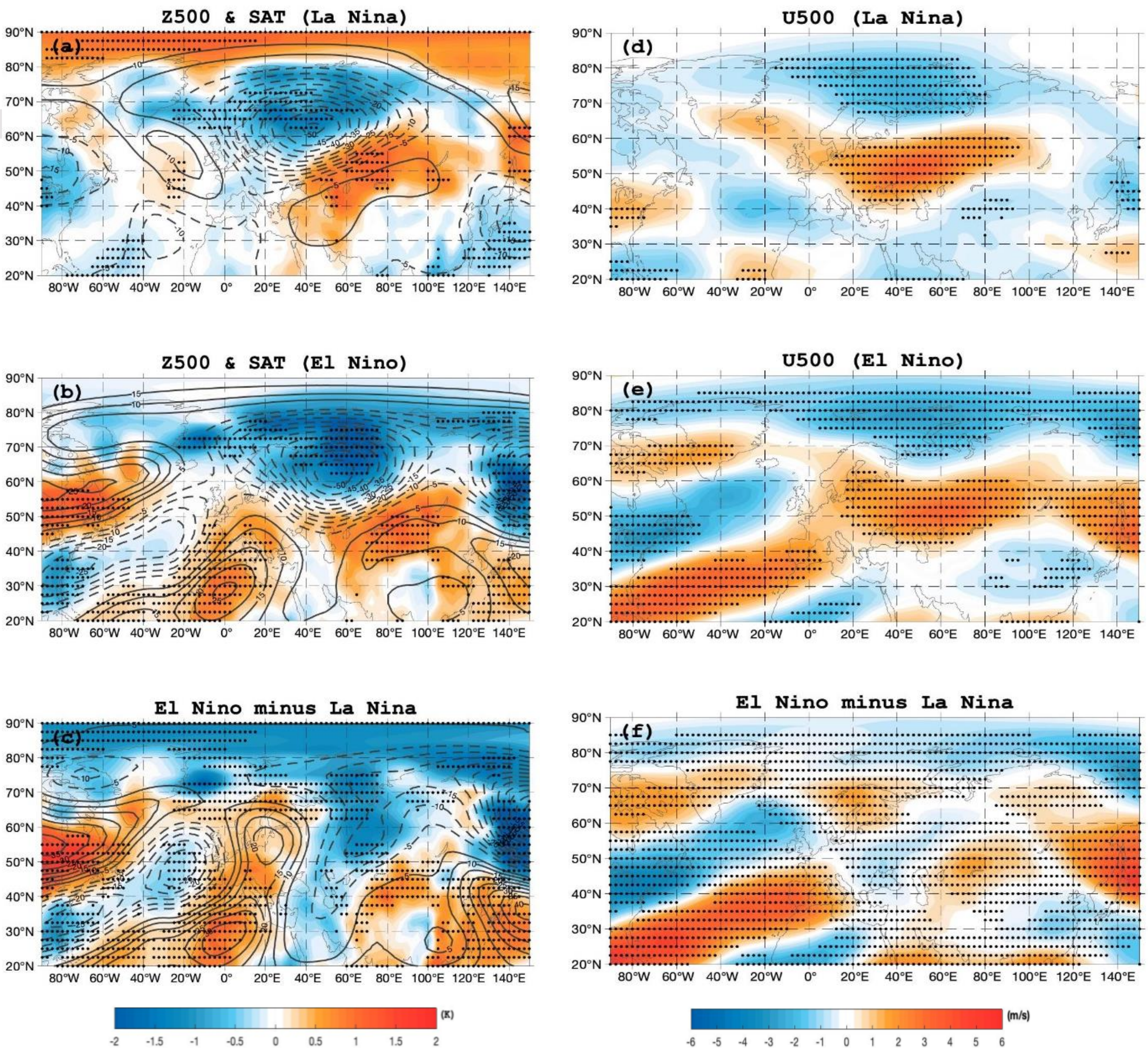
Z500 & SAT (La Nina)
(a)
U500 (La Nina)
(d)
Z500 & SAT (El Nino)
(b)
U500 (El Nino)
(e)
El Nino minus La Nina
(c)
El Nino minus La Nina
(f)
90°N
80°N
70°N
60°N
50°N
40°N
30°N
20°N
80°W 60°W 40°W 20°W 0° 20°E 40°E 60°E 80°E 100°E 120°E 140°E
(K)
-2 -1.5 -1 -0.5 0 0.5 1 1.5 2
(m/s)
-6 -5 -4 -3 -2 -1 0 1 2 3 4 5 6